AD-A190 699 HIGH TEMPERATURE OXIDATION AND ELECTROCHEMICAL STUDIES 1/1
RELATED TO HOT CORROSION(U) PENNSYLVANIA STATE UNIV
UNIVERSITY PARK DEPT OF MATERIALS SCI D KIM ET AL.
UNCLASSIFIED DEC 87 N00014-86-K-0133 F/G 7/4 NL

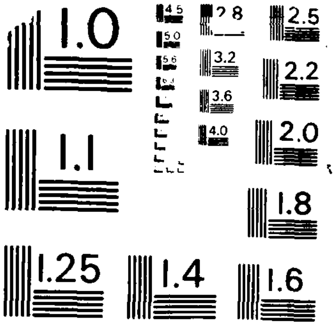

MICROCOPY RESOLUTION TEST CHART
NATIONAL BUREAU OF STANDARDS-1963-

4

College of Earth and Mineral Sciences

PENNSTATE

1 8 5 5

ANNUAL TECHNICAL REPORT

December 1987

OFFICE OF NAVAL RESEARCH

Contract NO. N0014-86-K-0133

HIGH TEMPERATURE OXIDATION AND ELECTROCHEMICAL STUDIES RELATED TO HOT CORROSION

D-H. Kim, J. Patton and G. Simkovich

Department of Materials Science and Engineering
The Pennsylvania State University
University Park, Pennsylvania 16802

PENN STATE
College of Earth and Mineral Sciences

Undergraduate Majors

Ceramic Science and Engineering, Fuel Science, Metals Science and Engineering, Polymer Science; Mineral Economics; Mining Engineering, Petroleum and Natural Gas Engineering; Earth Sciences, Geosciences; Geography; Meteorology.

Graduate Programs and Fields of Research

Ceramic Science and Engineering, Fuel Science, Metals Science and Engineering, Polymer Science; Mineral Economics; Mining Engineering, Mineral Processing, Petroleum and Natural Gas Engineering;
Geochemistry and Mineralogy, Geology, Geophysics; Geography; Meteorology.

Universitywide Interdisciplinary Graduate Programs Involving EMS Faculty and Students

Earth Sciences, Ecology, Environmental Pollution Control Engineering, Mineral Engineering Management, Solid State Science.

Associate Degree Programs

Metallurgical Engineering Technology (Shenango Valley Campus).

Interdisciplinary Research Groups Centered in the College

C. Drew Stahl Center for Advanced Oil Recovery, Center for Advanced Materials, Coal Research Section, Earth System Science Center, Mining and Mineral Resources Research Institute, Ore Deposits Research Group.

Analytical and Characterization Laboratories (Mineral Constitution Laboratories)

Services available include: classical chemical analysis of metals and silicate and carbonate rocks; X-ray diffraction and fluorescence; electron microscopy and diffraction; electron microprobe analysis; atomic absorption analysis; spectrochemical analysis; surface analysis by secondary ion mass spectrometry (SIMS); and scanning electron microscopy (SEM).

U.Ed. 87-1027
Produced by the Penn State Department of Publications

REPORT DOCUMENTATION PAGE

READ INSTRUCTIONS BEFORE COMPLETING FORM

1. REPORT NUMBER
Annual Technical Report

2. GOVT ACCESSION NO.

3. RECIPIENT'S CATALOG NUMBER

4. TITLE (and Subtitle)
High Temperature Oxidation and Electrochemical Studies Related to Hot Corrosion

5. TYPE OF REPORT & PERIOD COVERED
Annual Technical Report

6. PERFORMING ORG. REPORT NUMBER

7. AUTHOR(s)
D-H. Kim, J. Patton and G. Simkovich

8. CONTRACT OR GRANT NUMBER(s)
N0014-86-K-0133

9. PERFORMING ORGANIZATION NAME AND ADDRESS
Metallurgy Program, 209 Steidle Building
The Pennsylvania State University
University Park, PA 16802

10. PROGRAM ELEMENT, PROJECT, TASK AREA & WORK UNIT NUMBERS

11. CONTROLLING OFFICE NAME AND ADDRESS
Metallurgy Branch
Office of Naval Research
Arlington, VA 22217

12. REPORT DATE

13. NUMBER OF PAGES

14. MONITORING AGENCY NAME & ADDRESS (if different from Controlling Office)

15. SECURITY CLASS. (of this report)

15a. DECLASSIFICATION/DOWNGRADING SCHEDULE

16. DISTRIBUTION STATEMENT (of this Report)

17. DISTRIBUTION STATEMENT (of the abstract entered in Block 20, if different from Report)

18. SUPPLEMENTARY NOTES

19. KEY WORDS (Continue on reverse side if necessary and identify by block number)

20. ABSTRACT (Continue on reverse side if necessary and identify by block number)

This report covers some of the results attained during the past year concerning attempts to elucidating the mechanism(s) at hot corrosion processes.

AC impedance tests and Wagner-Hebb type polarization measurements on pure Na_2SO_4 at 900°C were performed as a function of Na_2O activities. These results, to be published in an Electrochem. Soc. Proceedings showed that the conductivities of the pure Na_2SO_4 were of the order of 2.57×10^{-1} $(\text{ohm-cm})^{-1}$ and varied only slightly with Na_2O activity changes. From the

DD FORM 1 JAN 73 1473 EDITION OF 1 NOV 65 IS OBSOLETE
S/N 0102-014-6601

. 25'i

Wagner-Hebb type polarization measurements on the pure Na_2SO_4 it was found that electron conductivity was much higher than electron hole conductivity. The transport numbers calculated were $t_O = 3.7 \times 10^{-4}$ and $t_\oplus = 7.0 \times 10^{-6}$.

Additional tests were conducted to determine (1) the effect of height of Na_2SO_4 melts, (2) the effect of electronic short circuiting the Na_2SO_4 melts with gold wires and (3) the effect of pre-saturating the salt melt with corrosion products in the hot corrosion process. Basically, these tests showed that neither ionic nor electronic transport in the bulk melt controls the hot corrosion process. However, the amount of Na_2SO_4 present, which is directly proportional to the height of the melt, does affect the rate of corrosion. This was demonstrated by the decrease in rate observed when the melt was pre-saturated with the corrosion products.

(Sodium Sulfate

This report is divided into into two parts. Part I is a copy of a paper which will be published in the Proceedings of the Electrochemical Society's symposium on "High Temperature Materials/Corrosion-High Temperature Materials Chemistry IV". This section deals with some of the transport properties of pure Na_2SO_4 at 900°C.

Part II covers the work related to the effects of altering the transport properties of the Na_2SO_4 melts. Such alterations were attained by varying the height of the melt, by electronically short-circuiting the melt and by prior saturation of the melt with the corrosion products.

PART I

ELECTRICAL CONDUCTION IN MOLTEN SODIUM SULFATE

D-H Kim and G. Simkovich
The Pennsylvania State University
206 Steidle Building
University Park, PA 16802

Abstract

Wagner-Hebb type polarization experiments and total electrical conductivity measurements by A.C. impedance technique were carried out on a pure Na_2SO_4 melt as a function of Na_2O activity at 1173 K.

It was observed that the total electrical conductivity of pure Na_2SO_4 was of the order of 2.57×10^{-1} $(\text{ohm-cm})^{-1}$ and varied only slightly with changes in the activity of Na_2O. From the Wagner-Hebb type D.C. polarization experiments on pure Na_2SO_4, the electron conductivity was shown to be much greater than the electron hole conductivity over the entire range of Na_2O activity.

Introduction

In general, alkali metals and alkaline earth metals, which commonly exist as impurities in the environment and/or fuel, react with sulfur oxides formed during the combustion process providing sulfates that can be deposited on the alloy surface. These deposits are usually, or become molten, at the operating temperatures of gas turbines or jet engines and cause enhanced metal deterioration due to oxidation/sulfidation reactions, generally called hot corrosion.

The mechanism of hot corrosion is rather well accepted as that of a dissolution process of the protective alloy oxides in the presence of the salt melts. One of the primary salts leading to this hot corrosion process is Na_2SO_4 which melts at about 884°C.

Since little is known about the electronic transport properties in molten Na_2SO_4, this study was concerned with obtaining such information with the thought of aiding in the elucidation of the mechanism of the process. Thus, Wagner-Hebb type polarization studies (1,2) as well as total electrical conductivity measurement by an A.C. impedance technique were carried out to evaluate the transport numbers of the electronic species in the melt.

The total electrical conductivity can be obtained by measuring the resistance of the melt by the relation:

$$\sigma = \frac{1}{R}\left(\frac{L}{A}\right) \qquad [1]$$

where σ : conductivity of the melt $(\text{ohm-cm})^{-1}$
R : resistance (ohm)
L/A : cell constant (1/cm)

The cell constant was obtained by conducting an A.C. impedance measurement of a standard 0.1 N KCl solution at room temperature under identical conditions to those utilized for the cell at high temperature. The cell constant was then calculated by multiplying the known specific conductivity (3).

An A.C. impedance technique was utilized to measure the resistance of pure molten Na_2SO_4 since Na_2SO_4 melts showed some polarization effects at the electrodes in our preliminary D.C. experiments.

The parameters which characterize the corrosion behaviors of the electrodes and/or the melts can be determined from a plot of the real impedance part, Z', versus wZ" where Z" is the imaginary part of the impedance and the frequency f is expressed as $w = 2\pi f$ (4). The frequency range employed was from 5 to 10^5 Hz. A plot of Z' versus wZ" according to

$$Z' = R_\Omega + R_p - R_p C w Z'' \qquad [2]$$

where R_Ω is the resistance of the electrolyte
R_p is the polarization resistance
C is the double layer capacitance

leads to a straight line with a slope of $-R_p C$ and an intercept of $R_p + R_\Omega$ for $w \rightarrow 0$ and at high frequencies, Z' approaches R_Ω (4). A Bode plot (log Z versus log w) was also employed to check the data obtained from the above method.

The idea that an appropriate choice of electrodes enables the suppression of either ionic or electronic transport in a galvanic cell provides the basis for the polarization technique. This technique has been extensively employed to investigate electronic conductivity in ionic solids (5-10) and has also been applied to a few molten systems (11-13).

Wagner (1) has derived the appropriate relation for the polarization conditions from transport theory. It states that, under steady state conditions, the total current due to passage of electronic species through the polarization cell is given by

$$I_{elect} = I_\theta + I_\oplus$$

$$= \frac{RTA}{LF}\left\{\sigma^o_\theta\left[1-\exp\left(-\frac{EF}{RT}\right)\right]+\sigma^o_\oplus\left[\exp\left(\frac{EF}{RT}\right)-1\right]\right\} \qquad [3]$$

where $I_\theta, I_\oplus$: electron and electron hole currents, respectively
$\sigma_\theta{}^\circ, \sigma_\oplus{}^\circ$: electron and electron hole conductivity, respectively
E : applied voltage
F : Faraday constant
R : gas constant
T : temperature (K)
L/A : cell constant.

In the derivation of equation (3) it is assumed (12,13) that

(i) excess electrons and holes follow the laws of ideal dilute solutions,
(ii) their mobilities are independent of concentrations,
(iii) the change in the concentration of atomic defects arising from thermal disorder with variation in the metal to nonmetal ratio is small,
(iv) convection in the melt is negligible.

The division of equation (3) by [1-exp(-EF/RT)] and rearrangement gives

$$I_{elect}\left\{\frac{LF}{RTA}\,\frac{1}{\left[1-\exp\left(-\frac{EF}{RT}\right)\right]}\right\} = \sigma^o_\theta + \sigma^o_\oplus \exp\left(\frac{EF}{RT}\right) \qquad [4]$$

and a plot of the left hand side of equation (4) versus exp (EF/RT) gives $\sigma_\theta{}^\circ$ as the intercept and $\sigma_\oplus{}^\circ$ as the slope. These values, combined with total electrical conductivity results, permit the evaluation of the transport numbers of each electronic carrier in the molten Na_2SO_4.

In the present work, steady state currents were measured on the polarization cell for different applied voltages. The applied voltage was always below the decomposition potential so that only electronic conduction is allowed.

Experimental Procedure

The thermodynamic activity of Na_2O in the Na_2SO_4 salt melt was set utilizing the following thermodynamic data.

(i) Gas Preparation

From the thermodynamic considerations

$$Na_2SO_4(l) = Na_2O(s) + SO_2 + 1/2\ O_2 \qquad [5a]$$

$$\Delta G^o_1 = 150300 - 51.82\ T\ (\text{cal}) \qquad [5b]$$

with the equilibrium condition

$$K_1 = \frac{a_{Na_2O}\, P_{SO_2}\, P^{1/2}_{O_2}}{a_{Na_2SO_4}} = \exp\left(-\frac{\Delta G^o_1}{RT}\right) \qquad [5c]$$

$$a_{Na_2O} = \frac{\exp\left(-\frac{\Delta G_1^o}{RT}\right) a_{Na_2SO_4}}{P_{SO_2}\ P_{O_2}^{1/2}} \qquad [5d]$$

and

$$ZnSO_4 = ZnO + SO_2 + 1/2\ O_2 \qquad [6a]$$

$$\Delta G_2^o = 78300 - 63.81\ T\ (cal) \qquad [6b]$$

$$K_2 = \frac{a_{ZnO}\ P_{SO_2}\ P_{O_2}^{1/2}}{a_{ZnSO_4}} = \exp\left(-\frac{\Delta G_2^o}{RT}\right) \qquad [6c]$$

If the activities of ZnO and $ZnSO_4$ are assumed to be unity, then equation [6c] becomes

$$K_2 = P_{SO_2}\ P_{O_2}^{1/2} = \exp\left(-\frac{\Delta G_2^o}{RT}\right) \qquad [6d]$$

The substitution of equation [6d] into [5d] allows the evaluation of the activity of Na_2O as a function of temperature, i.e.,

$$a_{Na_2O} = \exp\left(\frac{\Delta G_2^o - \Delta G_1^o}{RT}\right) a_{Na_2SO_4} \qquad [7]$$

Now, $\Delta G_1°$ (14) and $\Delta G_2°$ (15) are given by equation [5b] and [6b], respectively and the activity of Na_2SO_4 is assumed to be unity when a pure Na_2SO_4 melt is involved.

Thus, atmospheres of $SO_2 + O_2$ employed to vary the activity of Na_2O in the melt were obtained by flowing an inert gas, helium, over $ZnSO_4$/ZnO mixtures held at constant temperature in a furnace separate from the cell furnace. The helium gas was passed through a series of conventional purifiers. The $ZnSO_4$ and ZnO powders were supplied by J. T. Baker Chemical Company.

(ii) Total Conductivity Measurements

A.C. impedance measurements were involved to obtain polarization free total electrical conductivity. As shown in Figure 1, the three electrode system was utilized for the A.C. impedance measurements. The reference electrode was a silver wire immersed into a 10 m/o Ag_2SO_4/Na_2SO_4 melt contained in the Na ion conducting membrane, mullite tube (0.7 cm I.D.) (16). The working electrode and counter electrode were pure gold wires. Platinum wires welded to those electrodes were employed as leads to connect to the EG&G Model 273 potentiostat coupled with Model 5208 Lock-In amplifier.

The crucible utilized for these experiments was pure gold which is relatively inert to the aggressive salt. The height of the molten salt in the gold crucible was 2.54 cm and Au electrodes were immersed into the melt 1.27 cm from the bottom.

The quartz reaction chamber containing the gold crucible was heated by a resistance wound Kanthal furnace. The temperature of 1173±1 K in the hot zone of the furnace was monitored by a Pt-Pt 10% Rh thermocouple and regulated by an Omega Model 149-713 Temperature Controller. A variac limited the incoming voltage for the cell furnace.

(iii) Polarization Cell

As shown in Figure 2.a, the constant voltage was supplied to the polarization cell via a Keithley 260 Nanovolt source. A Keithley Digital Multimeter, Model 177 was used as an ammeter. A Solid State Electrometer, Model 610C was utilized to check the actual voltage on the polarization cell. An alumina shield was involved (Figure 2.b), so that the electronic species could travel from the edge of one electrode to that of the other.

The Na_2SO_4 samples involved in these experiments were an anhydrous ultrapure Na_2SO_4 (99.999%) supplied by Alfa Products.

Results and Discussion

Total electrical conductivities of a pure Na_2SO_4 at 1173 K are depicted in Figure 3 as a function of the activity of Na_2O in the melt. The total electrical conductivities remain rather constant regardless of the changes in Na_2O activities. Figure 3.a displays this conductivity on a more sensitive conductivity scale. The total electrical conductivity of a pure Na_2SO_4 melt was averaged as 0.257 $(\text{ohm-cm})^{-1}$ which is about one order of magnitude smaller than the literature values (17,18). This discrepancy is most probably caused by the facts that the previous investigators had: (1) a relatively impure Na_2SO_4, (2) a reaction between their quartz capillary and molten sodium sulfate, and (3) a reaction with their Pt electrodes. We have observed significant deterioration of quartz crucibles used to contain the Na_2SO_4 melts in our preliminary work and that there was reaction of Na_2SO_4 melts with Pt electrodes.

From the Wagner-Hebb type polarization measurements on pure Na_2SO_4 melt at 1173 K the partial conductivities of electrons and electron holes were obtained and are depicted in Figure 4. It can be seen that electron conduction in pure Na_2SO_4 is considerably larger than that of electron holes over the entire Na_2O activity range. Furthermore, it is noted that both electron and electron hole conductivities remain relatively constant regardless of the changes in Na_2O activities.

Utilizing the values of total electrical conductivities and electronic conductivities provides the transport numbers of electronic species; these are plotted in Figure 5 for a pure Na_2SO_4 melt. The transport numbers of electrons are of the order of 10^{-4} while those of electron holes are of the order of 10^{-6}. Such indicates that the electronic conduction in a pure Na_2SO_4 melt arises primarily via electron transport over the whole Na_2SO_4 activity range. The transport numbers of electronic species in molten salts have not been measured extensively but the few that have been measured are somewhat larger than those determined in this study, e.g., $t_{\ominus} = 3 \times 10^{-3}$ in the molten eutectic of LiCl-KCL at 450°C (18).

Summary and Conclusions

The main thrust of this experimental program was to obtain some of the transport properties in the aggressive molten salt Na_2SO_4. The total electrical conductivity measurements by A.C. impedance technique and Wagner-Hebb type polarization experiments provided the total electrical conductivity, electron conductivity, and electron hole conductivity of a pure Na_2SO_4 melt at 1173 K. From these measurements the transport numbers of electrons, $t_{\ominus}$, and electron holes, $t_{\oplus}$, were calculated as follows:

$$t_{\ominus} = 3.7 \times 10^{-4}; \; t_{\oplus} = 7.0 \times 10^{-6}$$

These experimental investigations have shown that a pure Na_2SO_4 melt has a somewhat low total electrical conductivity and that electronic conduction in the molten salt occurs primarily via the transport of electrons.

Ongoing investigations concerning the effect of impurities in the Na_2SO_4 melt of hot corrosion products are underway at this time.

Acknowledgments

We are most grateful to the ONR for their financial support under contract # N0014-86-K-0133 and the interest of our monitor, Dr. A. J. Sedriks.

References

1. C. Wagner, Proc. of Seventh Meeting of the Inter. Comm. on Thermo. and Kinetics of Eectrochem, (CITCE), Butterworth Scientific Publications, London, Vol. 7, p.361 (1957).

2. M. H. Hebb, J. Chem. Phys., 20, 185 (1952).

3. D. Dobos, "Electrochemical Data," published by the Elsevier Scientific Publishing Co., New York, p. 57 (1975).

4. F. Mansfeld, Corr.-NACE, 36, 301 (1981).

5. J. B. Wagner, Jr. and C. Wagner, J. Chem. Phys., 26, 1597 (1957).

6. A. Lingras and G. Simkovich, J. Phys. Chem. Solids, 39, 1225 (1978).

7. A. V. Joshi and J. B. Wagner, Jr., J. Phys. Chem. Solids, 33, 205 (1972).

8. A. V. Joshi and J. B. Wagner, Jr., J. Electrochem. Soc., 122, 1071 (1975).

9. D. Raleigh, J. Phys. Chem. Solids, 26, 329 (1965).

10. J. Sachoonman, A. Wolfert, and D. F. Untereker, Solid State Ionics, 11, 187 (1983).

11. R. J. Heus and J. J. Egan, J. Phys. Chem., 77, 1989 (1973).

12. R. J. Heus and J. J. Egan, in "Proceedings of International Symposium on Molten Salts," Electrochem. Soc., Pennington, NJ (1976), p. 523.

13. G. J. Reynolds, M.C.Y. Lee and R. A. Huggins, in "Proceedings of the Fourth International Symposium on Molten Salts," Electrochem. Soc., pv 84-2, Pennington, NJ (1984), p. 519.

14. D. R. Stull and H. Prophet, "JANAF Thermochemical Tables," NSRDS-NBS 37, U.S. Dept. Commer., Washington, D.C. (1971).

15. I. Barin, O. Knacke and O. Kubaschewski, "Thermochemical Properties of Inorganic Substances, Supplement," Springer-Verlag, Berlin and New York (1977).

16. D. A. Shores and R. C. John, J. Appl. Electrochem. 10, 275 (1980).

17. A. Josefson and A. Kvist, Z. Naturforsch., 24a, 466 (1969).

18. K. Matiasovsky, V. Danek and B. Lillebuen, Electrochim. Acta, 17, 463 (1972).

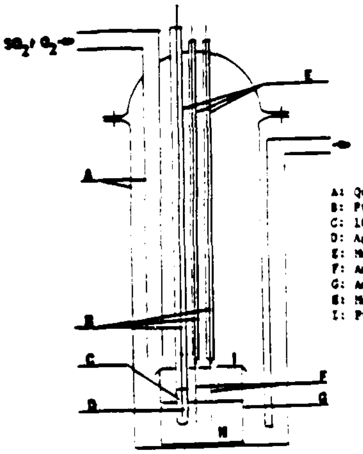

A: Quartz Tube
B: Pt Wires
C: 10 m/o Ag_2SO_4 / Na_2SO_4 melt
D: Ag Wire
E: Mullite Tube
F: Au Wires
G: Au Crucible
H: Molten Na_2SO_4
I: Pt Screen

Figure 1. Schematic Cell Arrangements for A.C. Impedance Measurements

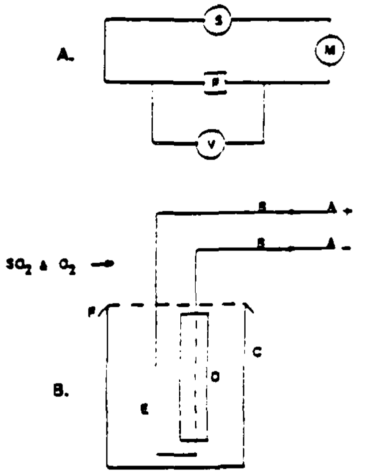

Figure 2 (a). Schematic Circuit Diagram for Polarization Experiments

Figure 2 (b). Polarization Cell Arrangements

A : Pt Lead Wires
B : Au electrodes
C : Au Crucible
D : Alumina Shield
E : Molten Sample
F : Pt Screen

M : Digital Multimeter
S : Power Source
P : Polarization Cell
V : High Impedance Voltmeter

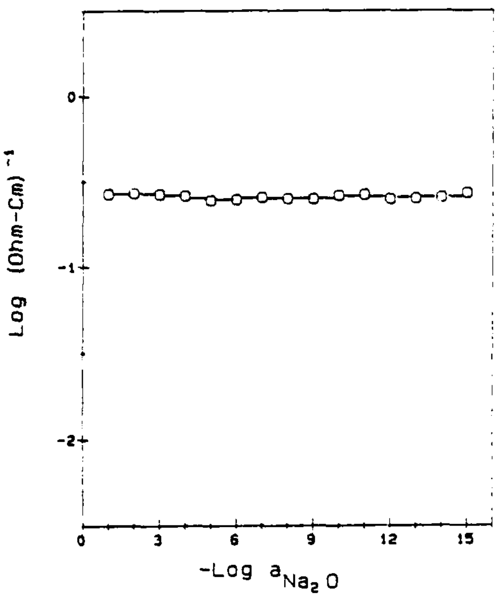

Figure 3. Log (total conductivity) versus Na_2O activity in a pure Na_2SO_4 melt at 1173 K

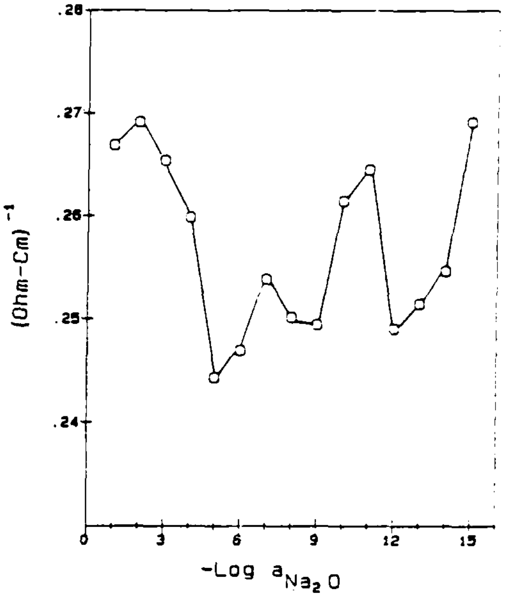

Figure 3 (a). Total Conductivity of a pure Na_2SO_4 melt as a function of Na_2O activities at 1173 K

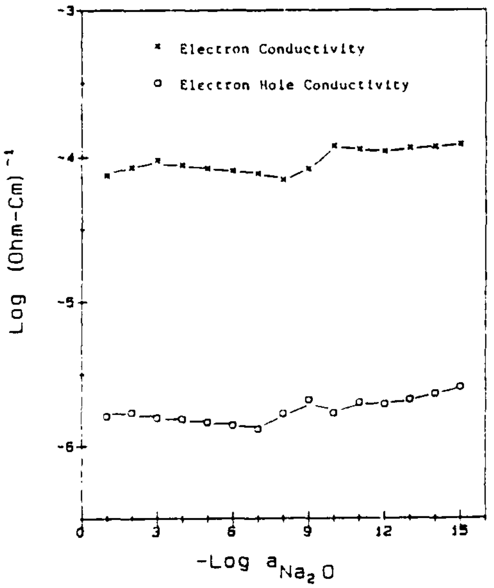

Figure 4. Electronic Conductivities in a pure Na_2SO_4 melt as a function of Na_2O activities at 1173 K

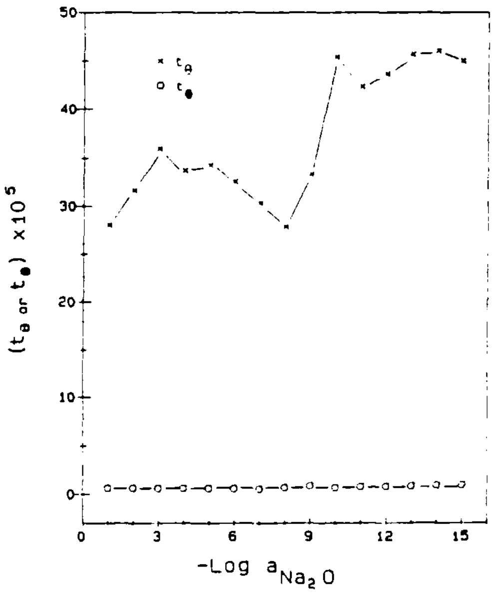

Figure 5. Transport Numbers of Electronic Species in a pure Na_2SO_4 melt as a function Na_2O activities at 1173 K

PART II

INTRODUCTION

The presence of molten salts in gas turbine engines may greatly accelerate high-temperature corrosion of the metals and alloys that comprise the engine. This phenomenon is generally termed "hot corrosion". In most evaluations, the molten salt is considered to be Na_2SO_4, which results from salt ingested into the engine and sulfur from the combustion of the fuel. Molten salt has to be present on the surface for accelerated corrosion to take place. Hot corrosion of nickel-base superalloys has been studied extensively because these alloys represent the most resistant materials available for high stress, high temperature use.

According to previous studies, the mechanisms of hot corrosion involve the dissolution of normally protective scales and the formation of an unprotective porous scale and metal sulfides next to the metal-salt interface. It would appear then that the initial reactions would necessarily involve first the formation of the metal oxides which in turn require the transport of oxygen through the liquid phase. Thus, the control of the process could manifest itself in either - (i) the gas-salt interface, (ii) diffusion through the gas-salt interface, (iii) diffusion through the bulk liquid. It can then be logically assumed that after the reaction between the oxide scale and the molten salt, the product layer would be involved in the control of the process.

To aid in the overall understanding of the hot corrosion process determination of a number of electrical transport processes in the Na_2SO_4 phase have been undertaken. The experiments conducted and the results are described in the following sections.

EXPERIMENTAL

High temperature hot corrosion studies were conducted on nickel, chromium and nickel-base superalloys. All experiments were carried out using cylindrical silica crucibles, which are relatively inert to the harsh salt environment. The crucible's use permitted the thickness of the Na_2SO_4 to be varied over a wide range. The thickness of the molten salt was determined by the consideration of the volume of the crucible and the density of the molten salt at 900°C.

The samples were prepared by first oxidizing the surfaces in a pure oxygen atmosphere at 1000°C for 12 hours. One surface was then ground to 600 grit while the remaining scaled surfaces were then coated with a thin layer of gold. This was done in order to confine the hot corrosion process to a single, clean reaction surface. The Na_2SO_4 was stored at 200°C for 48 hours before use in all experiments. Salt melts saturated with oxides were used in several experiments. These melts were equilibrated with the appropriate gas mixture before experimental use. In addition, several experiments were carried out using gold wires attached to the samples and extending through the melt.

The kinetics of the system were measured thermogravimetrically with an automatic recording balance. The specimens were connected to the balance by gold and platinum wire. Experiments were conducted with Na_2O activities of 6.3×10^{-16} and 5.01×10^{-11}. These conditions were maintained by flowing a gas mixture of O_2 and .15% SO_2 over platinum gauze prior to entering the quartz reaction chamber. A gas preheat zone was used to raise the gas temperature. This prevented the establishment of any temperature gradients between the gas and sample. To measure the reaction temperature a Pt-10%Rh thermocouple was attached outside the reaction chamber in the hot zone of the furnace.

RESULTS AND DISCUSSION

Hot Corrosion Studies of Transport Mechanisms

Hot corrosion experiments were performed using nickel, chromium and nickel-base superalloys as samples. These experiments examined changes in molten salt thickness, short-circuiting of the melt with gold wire, effects of presaturated melts and variations in the Na_2O activity.

Hot corrosion experiments were carried out with varying levels of Na_2SO_4. This was done in an effort to examine the role of bulk diffusion through the melt and its effect on the hot corrosion process. In Figures 1-3, results from experiments in which molten salt levels were varied from 0.5 cm to 2.0 cm are reported. It can seen from these figures that an increase in the height of the molten salt resulted in an increase in the weight gains per unit area of the corroding samples i.e. the kinetics of the system increase with increasing thickness. Therefore, one concludes that an increase in the diffusion path by increasing the thickness does not retard the hot corrosion process but rather accelerates the reaction. It can also be seen by comparing the results from the nickel and chromium samples that chromium appears less affected by the increase in the Na_2SO_4. The nickel-base superalloys are affected in a similar manner when subjected to the same conditions.

To further examine the transport through the bulk melt, gold wires were added to the samples. This was done in order to short circuit electronic transport the melt and to allow the evaluation of other transport species and their effect on the hot corrosion process. These experiments were also conducted as a function of Na_2SO_4 height and Na_2O activity. The results are presented in Figure 4. The kinetics of the system appear relatively unchanged by the addition of the gold wires. This seems to indicate that electronic transport through the melt is not rate determining. In addition, these results together with the salt height results imply that the gas-salt interface has very little control on the hot corrosion process.

Results from previous experiments show the kinetics of the system increase with salt thickness and transport through the bulk molten salt and the gas-salt interface has little or no effect on the reaction. Therefore, considering the possible role of the dissolution of the scale, it may be that the capacity of the Na_2SO_4 and its ability to accept the soluble product leads to an increase in weight gain per unit as the amount of salt increases. Thus, once the molten salt has been completely saturated, the hot corrosion process should be retarded. A series of experiments were run using both nickel and chromium samples with Na_2SO_4 saturated with their respective oxides. The results of these experiments are presented in Figure 5. The kinetics of the system appear to be drastically slowed down when compared to samples run in pure Na_2SO_4. This indicates that the hot corrosion process may be a function of the amount of Na_2SO_4 and thus, its ability to accept a soluble product.

In addition, experiments were run at an Na_2O activity of 5.01×10^{-11}. This corresponding change in activity led to a change in the kinetics of the system. Figure 6 shows a comparison of nickel and chromium samples run at both activities under various conditions. It can be seen from the results that there is a substantial difference in weight gain between the activities, but the effect of the varying thicknesses as well as the effect of saturating the salt melt with the appropriate oxides is still manifested in a decrease in kinetics.

CONCLUSIONS

The results attained are collectively providing a clarification of the hot corrosion process. We are able to conclude with respect to the hot corrosion process the following.

1. The gas-Na_2SO_4 melt interface is not rate controlling.
2. Diffusion in the boundary layers at the gas-melt interface is not rate controlling.
3. Electronic transport through the bulk melt is not rate controlling.
4. An increasing amount of Na_2SO_4 results in a greater weight gain per unit area for a given activity of Na_2O in the Na_2SO_4. This indicates that the capacity of the Na_2SO_4, prior to precipitation of products, to accommodate the products of the hot corrosion does influence the rate of reaction.
5. The above points appear to indicate that the processes occurring at or near the metal-salt interface seem to be of prime importance.

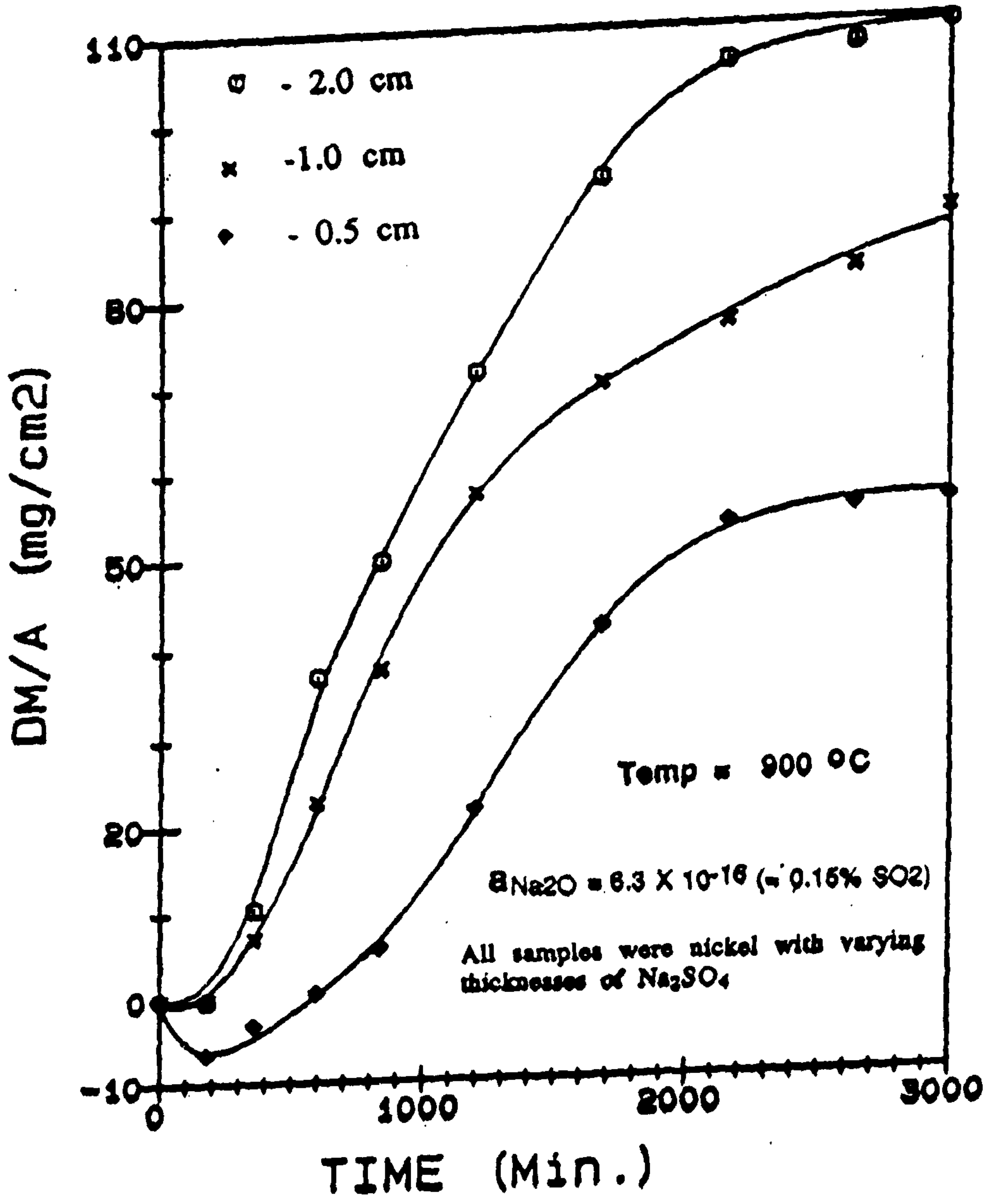

Figure 1. Weight gain as a function of Na_2SO_4 thickness.

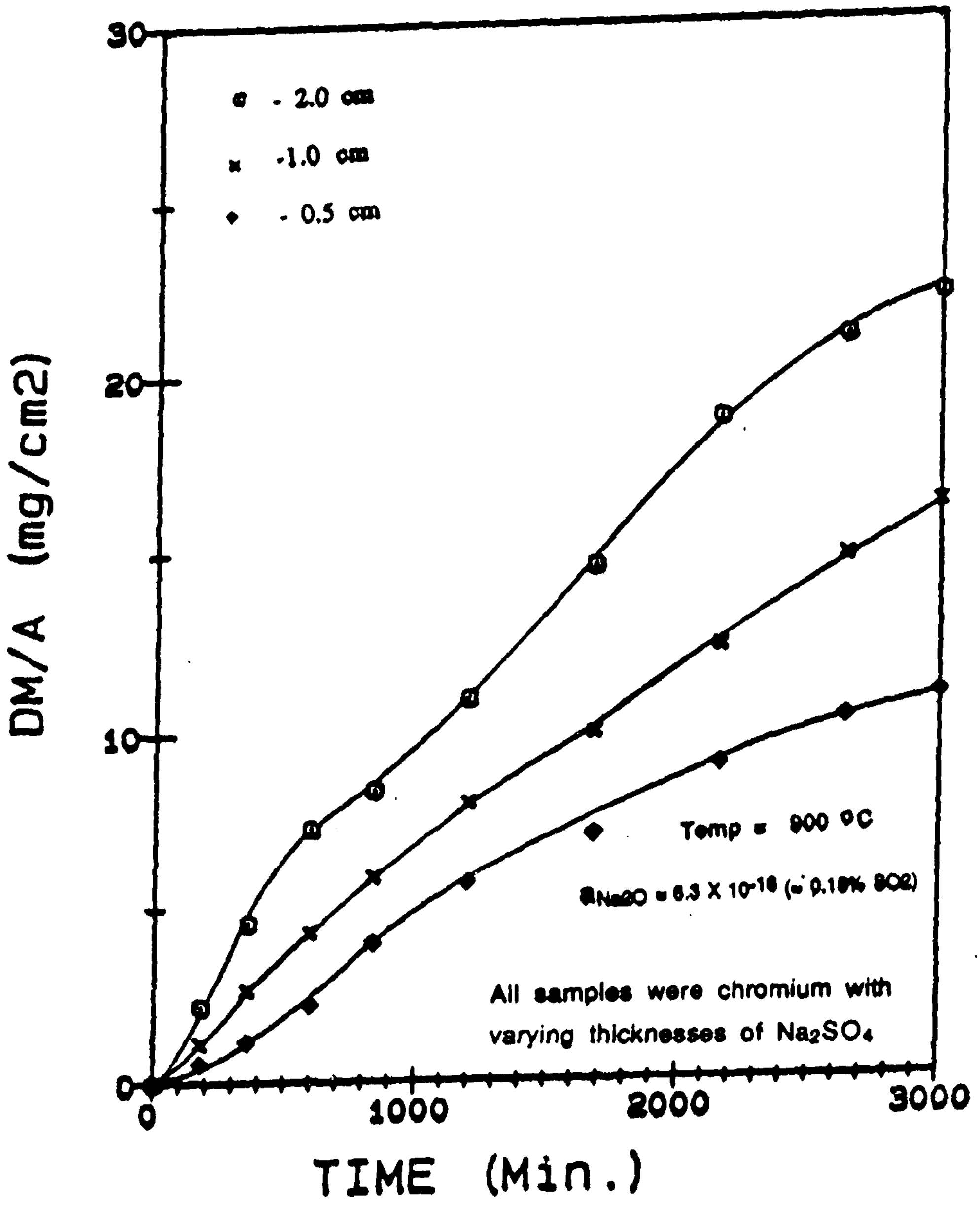

Figure 2. Weight gain as a function of Na_2SO_4 thickness.

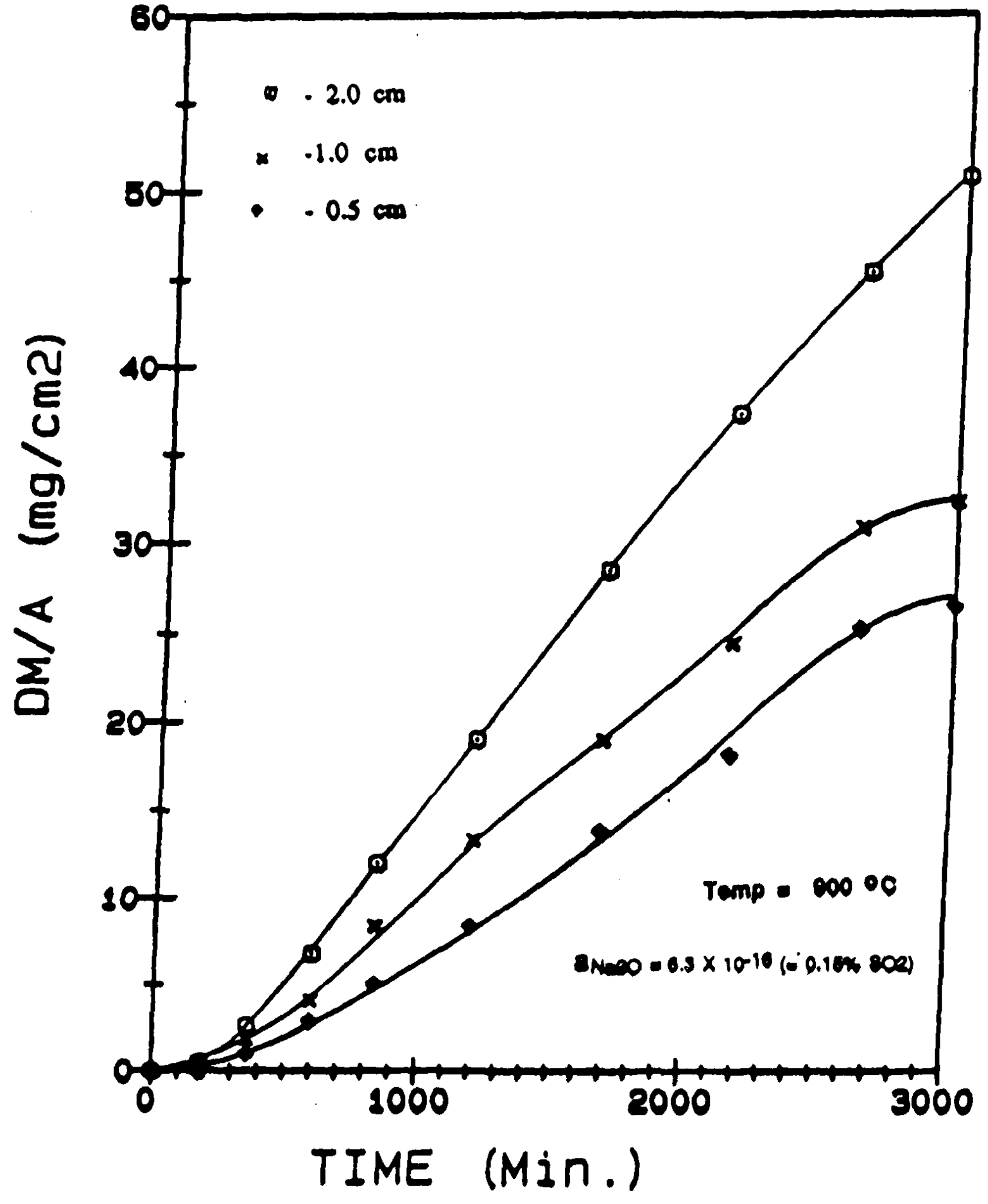

Figure 3. Weight gain of IN-713 as a function of Na_2SO_4 thickness.

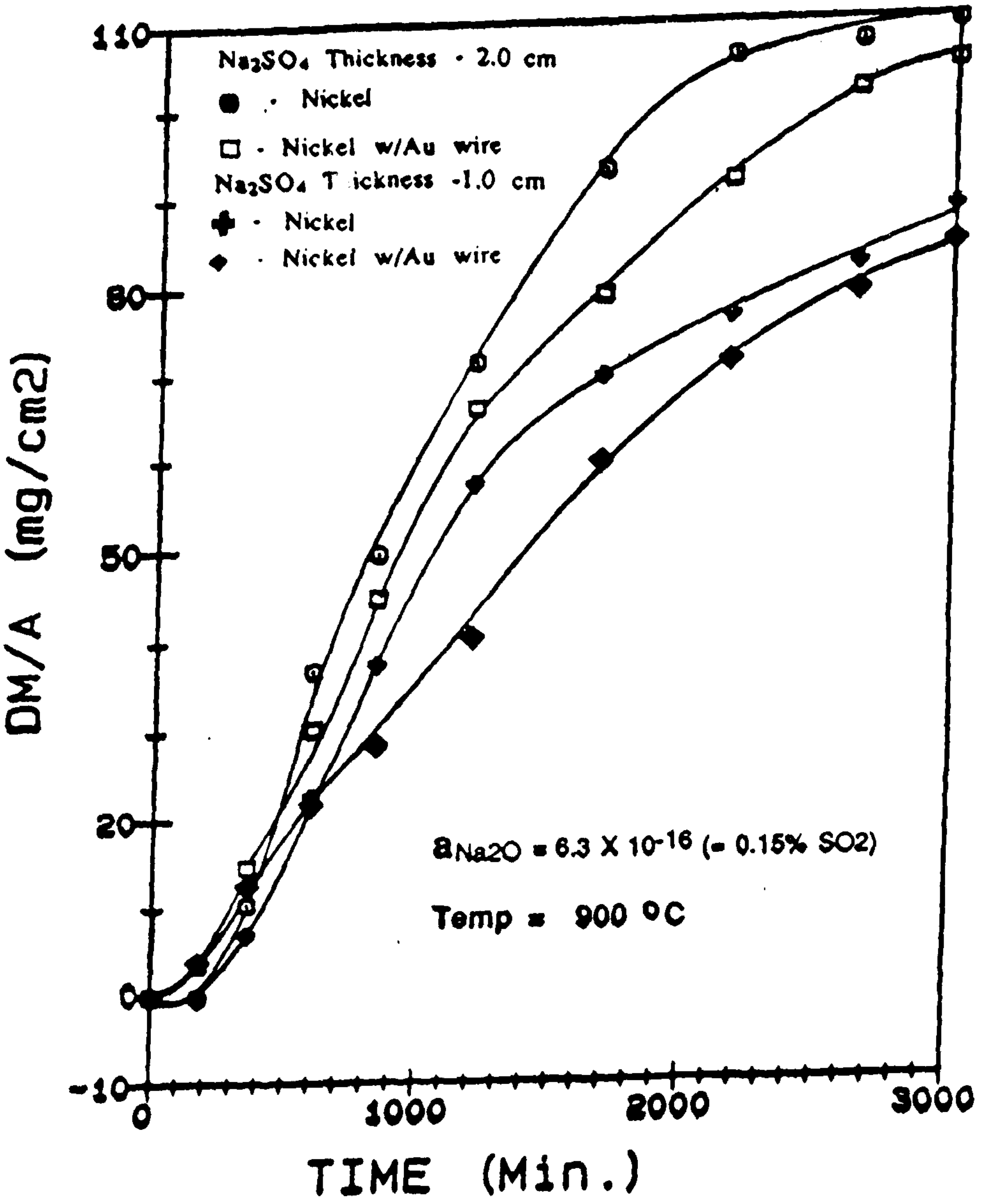

Figure 4. Nickel samples hot corroded with and without attached gold wires

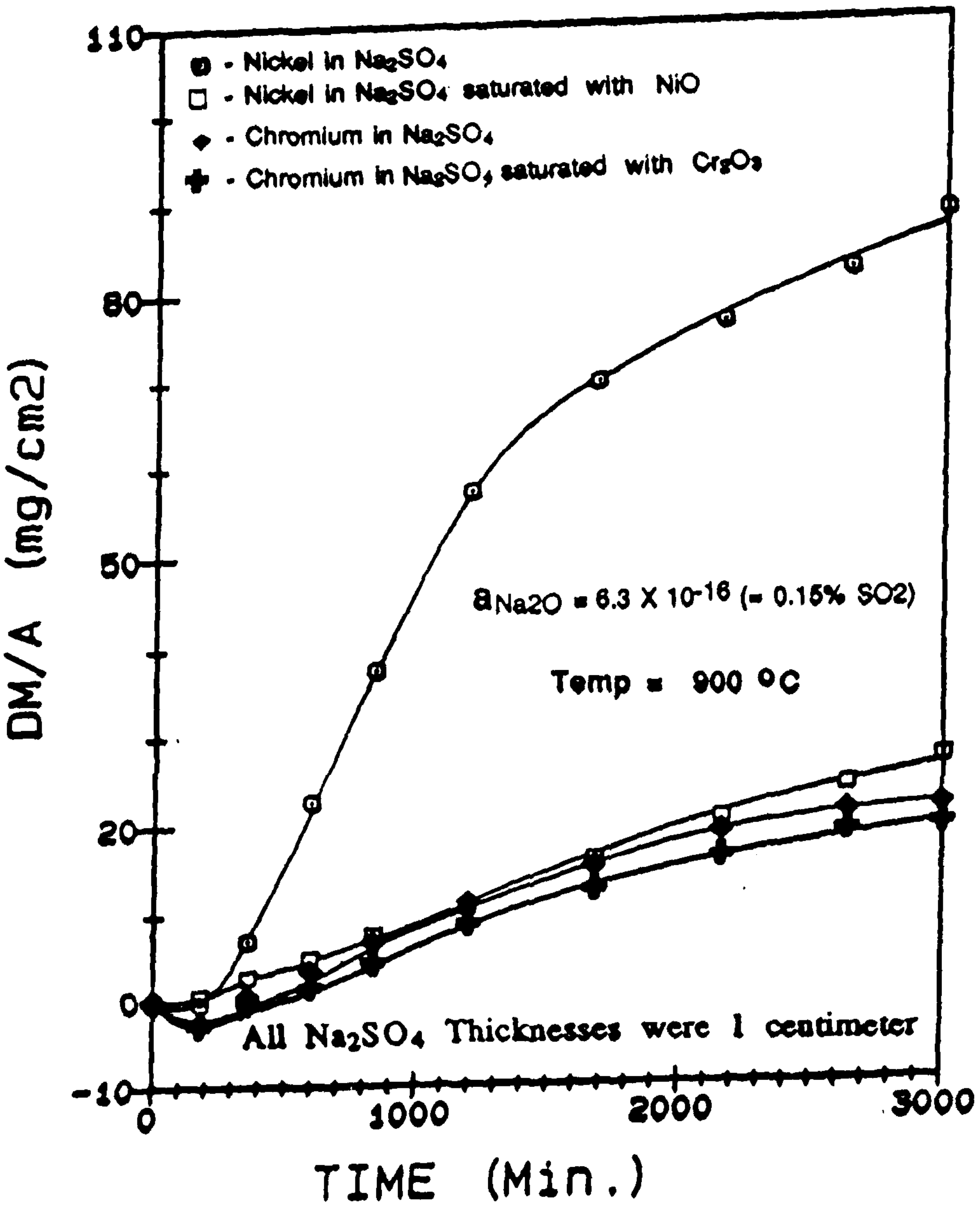

Figure 5. Weight gain as a function of time showing the effect of oxide saturated Na_2SO_4 on nickel and chromium samples.

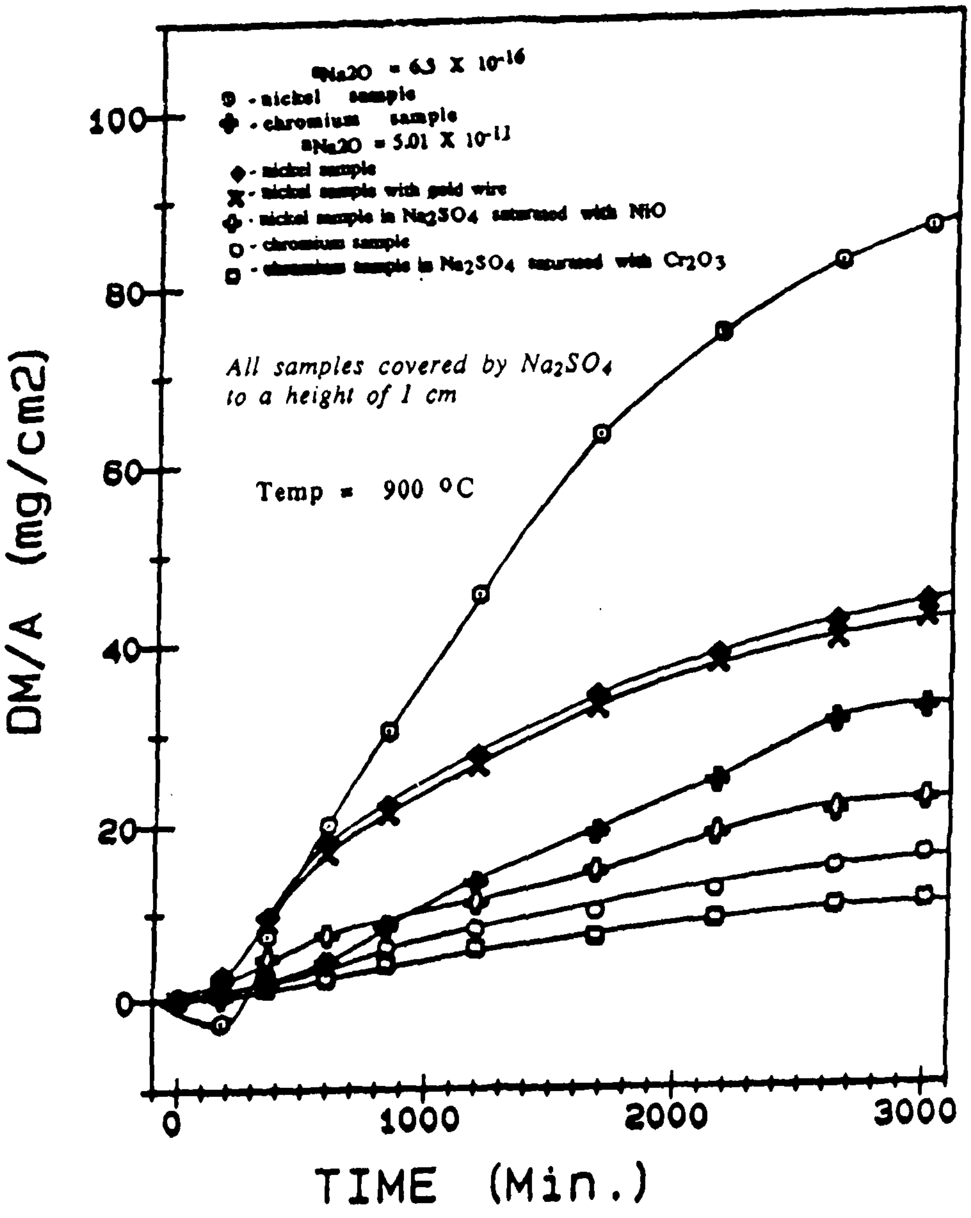

Figure 6. Weight gain as a function of varying Na_2O activities

036 (4315)

Supplemental Distribution List

Mar 1987

Prof. I.M. Bernstein
Dept. of Metallurgy and Materials Science
Carnegie-Mellon University
Pittsburgh, PA 15213

Prof. H.K. Birnbaum
Dept. of Metallurgy & Mining Eng.
University of Illinois
Urbana, Ill 61801

Prof. H.W. Pickering
Dept. of Materials Science and
Eng.
The Pennsylvania State
University
University Park, PA 16802

Prof. D.J. Duquette
Dept. of Metallurgical Eng.
Rensselaer Polytechnic Inst.
Troy, NY 12181

Prof. J.P. Hirth
Dept. of Metallurgical Eng.
The Ohio State University
Columbus, OH 43210

Prof. H. Leidheiser, Jr.
Center for Coatings and Surface Research
Sinclair Laboratory, Bld. No. 7
Lehigh University
Bethlehem, PA 18015

Dr. M. Kendig
Rockwell International - Science Center
1049 Camino Dos Rios
P.O. Box 1085
Thousand Oaks, CA 91360

Prof. R. A. Rapp
Dept. of Metallurgical Eng.
The Ohio State University
Columbus, OH 43210

Profs. G.H. Meier and F.S.Pettit
Dept. of Metallurgical and
Materials Eng.
University of Pittsburgh
Pittsburgh, PA 15261

Dr. W. C. Moshier
Martin Marietta Laboratories
1450 South Rolling Rd.
Baltimore, MD 21227-3898

Prof. P.J. Moran
Dept. of Materials Science & Eng.
The Johns Hopkins University
Baltimore, MD 21218

Prof. R.P. Wei
Dept. of Mechanical Engineering
and Mechanics
Lehigh University
Bethlehem, PA 18015

Prof. W.H. Hartt
Department of Ocean Engineering
Florida Atlantic University
Boca Raton, Florida 33431

Dr. B.G. Pound
SRI International
333 Ravenswood Ave.
Menlo Park, CA 94025

Prof. C.R. Clayton
Department of Materials Science
& Engineering
State University of New York
Stony Brook
Long Island, New York 11794

Prof. Boris D. Cahan
Dept. of Chemistry
Case Western Reserve Univ.
Cleveland, Ohio 44106

Dr. K. Sadananda
Code 6390
Naval Research Laboratory
Washington, D.C. 20375

Prof. M.E. Orazem
Dept. of Chemical Engineering
University of Virginia
Charlottesville, VA 22901

Mr. T.W. Crooker
Code 6310
Naval Research Laboratory
Washington, D.C. 20375

Prof. G.R. St. Pierre
Dept. of Metallurgical Eng.
The Ohio State University
Columbus, OH 43210

Prof. G. Simkovich
Dept. of Materials Science & Eng.
The Pennsylvania State University
University Park, PA 16802

Dr. E. McCafferty
Code 6310
Naval Research Laboratory
Washington, D. C. 20375

BASIC DISTRIBUTION LIST

Technical and Summary Reports 1985

Organization	Copies
Defense Documentation Center Cameron Station Alexandria, VA 22314	12
Office of Naval Research Department of the Navy 800 N. Quincy Street Arlington, VA 22217 Attn: Code 431	3
Naval Research Laboratory Washington, DC 20375 ATTN: Codes 6000 6300 2627	1 1 1
Naval Air Development Center Code 606 Warminster, PA 18974 ATTN: Dr. J. DeLuccia	1
Commanding Officer Naval Surface Weapons Center White Oak Laboratory Silver Spring, MD 20910 ATTN: Library	1
Naval Oceans Systems Center San Diego, CA 92132 ATTN: Library	1
Naval Postgraduate School Monterey, CA 93940 ATTN: Mechanical Engineering Department	1
Naval Air Systems Command Washington, DC 20360 ATTN: Code 310A Code 5304B	1 1
Naval Sea System Command Washington, DC 20362 ATTN: Code 05R	1

Organization	Copies
Naval Air Propulsion Test Center Trenton, NJ 08628 ATTN: Library	1
Naval Construction Battallion Civil Engineering Laboratory Port Hueneme, CA 93043 ATTN: Materials Division	1
Naval Electronics Laboratory San Diego, CA 92152 ATTN: Electron Materials Sciences Division	1
Naval Missile Center Materials Consultant Code 3312-1 Point Mugu, CA 92041	1
Commander David W. Taylor Naval Ship Research and Development Center Bethesda, MD 20084	1
Naval Underwater System Center Newport, RI 02840 ATTN: Library	1
Naval Weapons Center China Lake, CA 93555 ATTN: Library	1
NASA Lewis Research Center 21000 Brookpark Road Cleveland, OH 44135 ATTN: Library	1
National Bureau of Standards Washington, DC 20234 ATTN: Metals Science and Standards Division Ceramics Glass and Solid State Science Division Fracture and Deformation Div.	1 1 1

Naval Facilities Engineering
Command
Alexandria, VA 22331
ATTN: Code 03 1

Scientific Advisor
Commandant of the Marine Corps
Washington, DC 20380
ATTN: Code AX 1

Army Research Office
P. O. Box 12211
Triangle Park, NC 27709
ATTN: Metallurgy & Ceramics
Program 1

Army Materials and Mechanics
Research Center
Watertown, MA 02172
ATTN: Research Programs 1
Office

Air Force Office of Scientific
Research/NE
Building 410
Bolling Air Force Base
Washington, DC 20332
ATTN: Electronics & Materials
Science Directorate 1

NASA Headquarters
Washington, DC 20546
ATTN: Code RRM 1

Defense Metals and Ceramics
Information Center
Battelle Memorial Institute
505 King Avenue
Columbus, OH 43201 1

Metals and Ceramics Division
Oak Ridge National Laboratory
P.O. Box X
Oak Ridge, TN 37380 1

Los Alamos Scientific Laboratory
P.O. Box 1663
Los Alamos, NM 87544
ATTN: Report Librarian 1

Argonne National Laboratory
Metallurgy Division
P.O. Box 229
Lemont, IL 60439 1

Brookhaven National Laboratory
Technical Information Division
Upton, Long Island
New York 11973
ATTN: Research Library 1

Library
Building 50, Room 134
Lawrence Radiation Laboratory
Berkeley, CA 1

each unless otherwise indicated.

END
DATE
FILMED
DTIC
4/88